

# A Multiwavelength Review of PSR J0737–3039

Umang Mishra <sup>1</sup>

New York University Abu Dhabi

email: um339@nyu.edu

## Abstract.

This paper is a multi-wavelength review of the double pulsar binary PSR J0737–3039. (more will be added once the entire paper is finished).

**Keywords.** PSR J0737–3039, Double Pulsar Binary, General Relativity

## 1. Introduction

The double pulsar binary system J0737–3039 was discovered in 2004 using the Parkes 64-m radio telescope in New South Wales, Australia by Burgay et al. (2003). Right from its discovery, the pulsar binary was anticipated to be crucial towards better understanding of Post Newtonian formalism and gravitational waves. J0737–3039A is a millisecond pulsar with 22.7ms period, and its counterpart is a young unrecycled pulsar with a period of 2.77 s as summarized by Lyne (2006). While initially the system was only observed in the radio wavelengths for testing general relativity, observations were also performed using XMM Newton in soft X-ray. Some observations in gamma ray have also been performed. (More info on X-Ray and gamma later)

## 2. Radio Observations

### 2.1. The Discovery and the Parameters

Although the first observation was made by the Parkes 64-m at 1390Hz, better precision was obtained after interferometric observations were made using the Australia Telescope Compact Array(ATCA). The pulsar A of the system was found to be in a 2.4 hour eccentric orbit with eccentricity of 0.088 by Burgay et al. (2003). The ATCA measurements helped further measurement of parameters, giving a period of 22.699 ms for pulsar A. The period of pulsar B was found to be 2.8s by Lyne et al. (2004).

The periastron advance( $\dot{\omega}$ ) value was measured to be  $16.88\text{yr}^{-1}$  by the ATCA observations. This was the highest value of  $\dot{\omega}$  and was used to predict the masses of the pulsars in the system. Lyne et al. (2004) also measured other post Keplerian parameters, and found that the predictions of masses were accurate. The system was thus established as a highly relativistic double pulsar binary system ideal for testing relativistic gravity and DNS merger rates.

**Table 1.** A description of the six post-Keplerian parameters

$\dot{\omega}$	Periastron advance	Describes the rotation of the line connecting two pulsars at their closest approach to each other
$\gamma$	Gravitation Redshift and Time Dilation	Accounts for the apparent slowing of time due to general and special relativistic effects
$r$ and $s$	Shapiro Delay	These parameters define the Shapiro delay, which is delay in receiving signal due to space-time curvature
$dP_b/dt$	Orbital Decay	The rate of decrease of the orbital period due to emission of gravitational waves
$\Omega_{SO}$	Relativistic Spin Precession	Rate of the apparent precession of the pulsar about the orbital angular momentum that arises due to space-time curvature

## 2.2. The Double Neutron System(DNS) as a Testing Ground for General Relativity

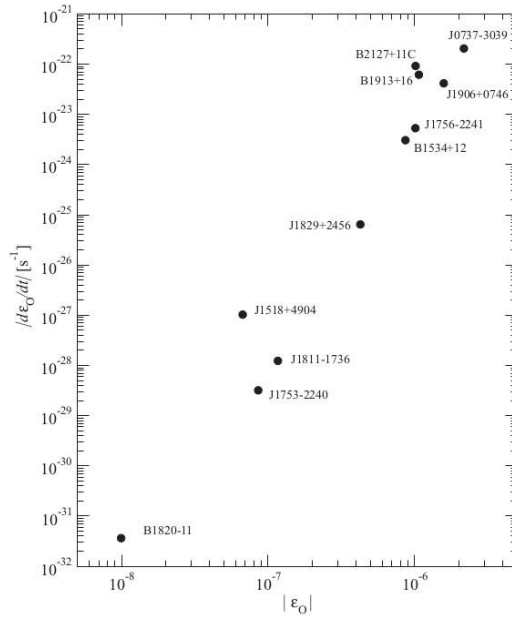


**Figure 1.** Orbital energy-energy loss diagrams for known and likely double neutron binaries.  $\epsilon_o$  is a direct measure for the strength of post-Newtonian effects in orbital dynamics. It can thus clearly be seen that J0737-3039 (top right) is the most suitable candidate for studying relativistic gravity. Image taken from Kramer and Wex (2009)

Usually, five Keplerian Parameters are sufficient to describe binary systems. These are:  $P_{orb}$ ,  $e$ ,  $\omega$ ,  $asini$ , and  $T_o$ . In case of strong gravitational interactions, such as in the case of a double neutron system, six additional parameters called the post-Keplerian parameters are required to fully describe the system due to relativistic effects that come into play. These are:  $\dot{\omega}$ ,  $\gamma$ ,  $r$ ,  $s$ ,  $dP_b/dt$ , and  $\Omega_{SO}$ . Since gravity is the only way stars in DNS interact, it makes them ideal candidates for studying relativistic gravity theories using these post-Keplerian parameters. The description of these parameters can be found in table 1.

**Table 2.** A comparison of measured and predicted values of the six post-Keplerian parameters. Values taken from Kramer and Wex (2009)

Parameter	Observed value	GR expectation	Ratio
$\dot{\omega}$ (deg yr <sup>-1</sup> )	16.899 47(68)	-	-
$\gamma_A(ms)$	0.3856(26)	0.38418(22)	1.0036(68)
$r_A$ ( $\mu s$ )	6.21(33)	6.153(26)	1.009(55)
$s$	0.999 74(39, +16)	0.999 87(48, +13)	0.999 87(50)
$dP_b/dt$	1.252(17)	1.24787(13)	1.003(14)
$\Omega_{SO}$ (deg yr <sup>-1</sup> )	4.77(+0.66, 0.65)	5.0734(7)	0.94(13)

As shown in figure 1, PSR J0737-3039 is the most suitable system for studying relativistic gravity. Each of the post-Keplerian(PK) parameters is related to the masses of the pulsars in the system in a unique way. With a system as J0737-3039, a ratio of stellar masses can be obtained from observations and plotted as a straight line according to the equation:

$$\frac{a_B \sin i}{a_A \sin i} = \frac{m_A}{m_b}$$

An intersection between this line and the curves plotted for each PK on a mass-mass plot could be used as a verification test for general relativity.

In the case of PSR J0737-3039, all five PK parameters can be measured for pulsar A. Since the equations for  $\dot{\omega}$ ,  $s$ , and  $dP_b/dt$  for general relativity are symmetric in masses, they will be the same for both pulsar A and pulsar B. Studies of eclipses of A allow for measurement of  $\Omega_{SO}$  for B. The mass-mass plot for these parameters, can be seen in figure 2. While all the experimental values agree within the error boundaries with the theoretical predictions, the best match is with Shapiro delay(with uncertainty of 0.05%). Exact values are listed in table 2.

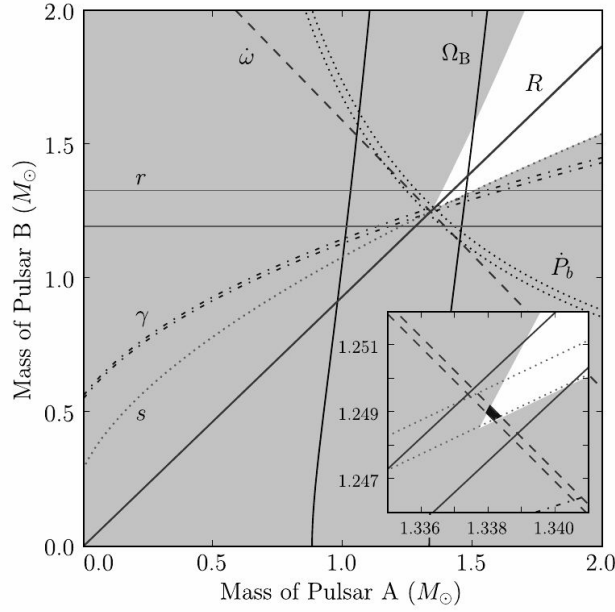


**Figure 2.** M-M graph to test general relativity using PK parameters for PSR J0737-3039.  
Taken from James et al. (2016)

### 2.3. Eclipsing of A and the Penetration of B's Magnetosphere

At conjunction, the line of sight of the two pulsars is within 0.15 ls of each other. As they further advance in their orbits, A is completely eclipsed by B and the line of sight of A sweeps through the magnetosphere of B. Lyne et al. (2004) suggested that studying the changes in radio transmission during this process can lead to understanding the physical conditions of B's magnetosphere, giving a better understanding of the plasma density and magnetic field structure. Analysis of flux densities (figure 3) revealed an occultation of A occurs that lasts around 20s or 30s. The spin-down energy loss of A being 3000 times greater than that of B, and the energy density of the relativistic wind from A being two orders of magnitude larger than B's, it was suggested that the wind from A will penetrate deep into B's magnetosphere. In fact, it was found that at radii greater than 40% of the light cylinder of B, the energy field of A dominates. Because of this, the penetration of wind from A into that of B was hypothesized to be dependent on their relative orientation. This dependence was cited as the cause for fluctuations in B's flux densities over time.

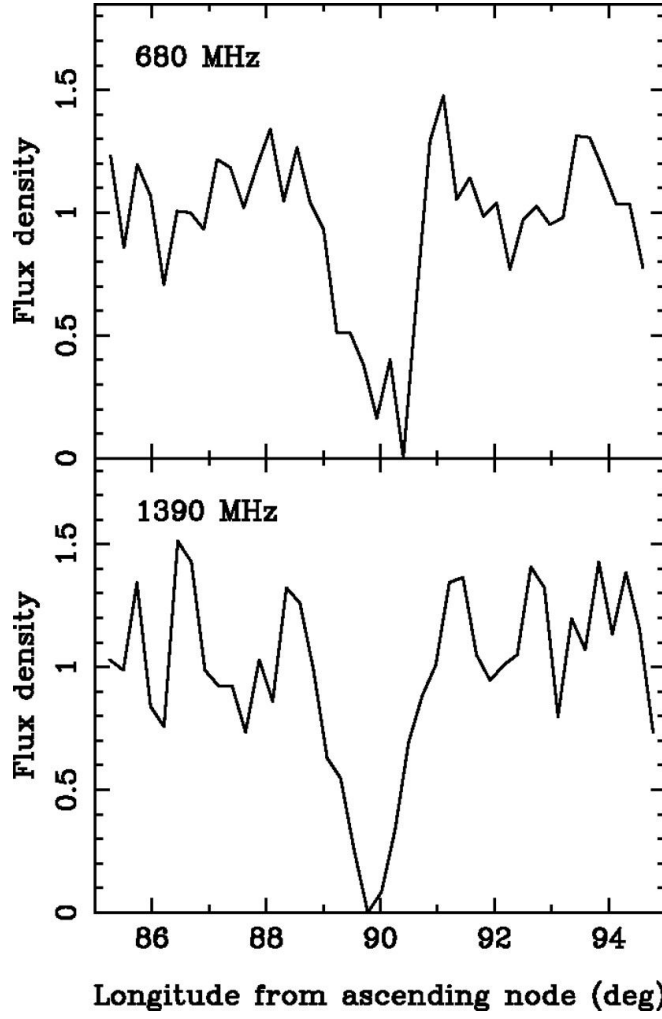


**Figure 3.** The variation in flux density of A (in arbitrary units) at 680 and 1390 MHz, around superior conjunction (i.e., longitude 90). The data are presented with 5-s time resolution and show the eclipse of the pulsar by the magnetosphere of B. Image and description taken from Lyne et al. (2004)

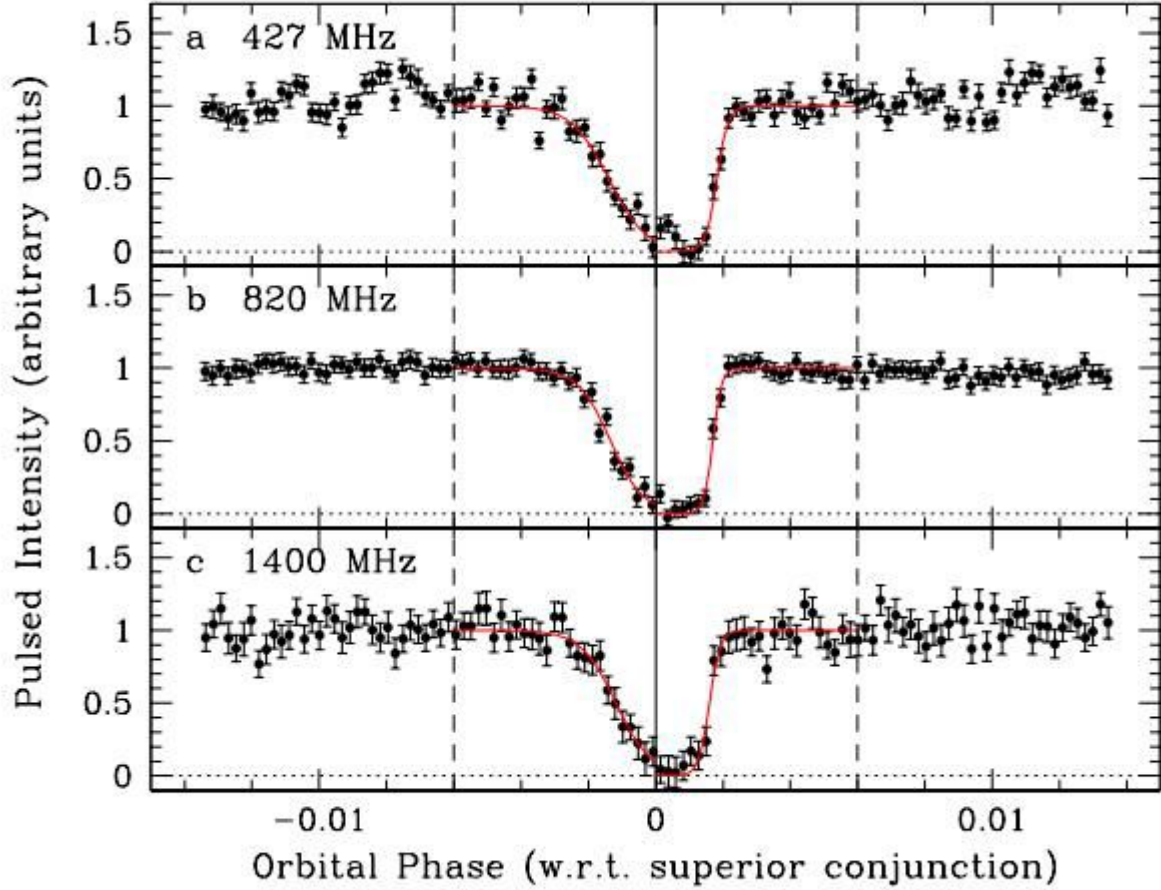


**Figure 4.** Pulsar A eclipse light curves. Each point represents 2 s of data; the shown curve is 4-min in duration, centered on conjunction. The x-axes are orbital phase with respect to conjunction. The y-axes are pulsed flux, normalized such that the pre-eclipse flux is unity. The panels are for (a) 427 MHz, (b) 820 MHz, and (c) 1400 MHz. The solid vertical line indicates conjunction and the horizontal dotted lines show 0 flux. Vertical dashed lines at  $\phi = 0.006, +0.006$  indicate the range of data fitted. The best-fit ingress and egress model curves are shown as solid lines. Figure and its description is from Kaspi et al., (2004)

Kaspi et al., (2004) observed the eclipsing of A in further detail using measurements from the Green Bank Telescope at 427, 820, and 1400 MHz. The light curves (figure 4) obtained showed that the eclipse ingress is longer than the eclipse egress. The observation also confirmed the eclipse model put forth by Arons et al. (2005) (Note that Aaron's paper was unpublished when GBT's results were published). A's wind confines B's magnetosphere on the side facing A, compressing it. While the part of B's magnetosphere opposite to the side facing A develops a magnetotail. The heating up of A's wind plasma by the bow shock developed was hypothesized to rise of synchrotron absorption, leading to A's eclipse. The rotation of B's magnetosphere was held accountable for the eclipse

asymmetries. It was also postulated that at frequencies around 5-10GHz, the eclipse will clear.

#### 2.4. Implications for the DNS Merger Rates

As already explained, PSR J0737-3039 has provided a rigorous testing ground for gravitation theories. However, it must be noted that the very first important result obtained from observations of stars in this system led to setting new limits on the DNS merger rates. A relativistic DNS system such as this is expected to result in a gravitational wave burst and a neutron star/black hole depending on the properties of stars in the system Lipunov (2004).

When PSR J0737-3039 was discovered, its lifetime was first found to be 85Myr. Since PSR B1913+16 and PSR B1534+12 were the highest contributors to merger rate calculations at that time, the lifetime and luminosity of PSR J0737-3039 was compared with these two stars. Since the lifetime of PSR B1913+16 was 300 My, PSR J0737-3039's discovery significantly affected the DNS merger rate estimates. With these considerations, Burgay et al. (2003) calculated that PSR J0737-3039 caused a decrease in DNS merger rates by one order of magnitude. So the DNS merger rate went from  $10^{-5} \text{ year}^{-1}$  to  $10^{-4} \text{ year}^{-1}$ .

### 3. Optical and Far Ultraviolet

The optical emission from pulsars, if any, is usually in the form of thermal radiation from the surface of the star, and/or non-thermal radiation from the magnetosphere(synchrotron radiation). However, only eighteen pulsars have been detected in the optical spectrum, of which, only seven have a pulsed emission in the optical. As a starting point, the luminosity of a pulsar due to synchrotron radiation can be estimated as being proportional to  $P^{-10}$ , as concluded by Pacini (1971) in his study of the Vela pulsar. Furthermore, the effects of duty cycle (as proposed by Pacini et. al (1987)) and orbital geometry also need to be taken into account. Pulsars thus have brightness on the order of 10, and are thus very faintly visible in optical region.

For PSR J0737-3039, the optical and UV observations followed extensive study of the system by XMM Newton in X-ray. There has been only one optical study of the system performed by Ferraro et. al . The observations by Ferraro et. al (2012) were made using the High Resolution Camera of the Advanced Camera for Surveys (ACS) on board the Hubble Space Telescope . The X-Ray studies by Pellizzoni et al. (2008) proposed three component model for the system- a power law and two blackbody components. The optical studies were done to confirm these findings . The images were taken using the F606W filter (roughly corresponding to Johnson's V filter) and F435W filter(roughly corresponding to Johnson's B filter). Since the pulsar is located around 4" from a bright star, the HRC coronagraph was used. The detection in optical was still not possible and only upper limits were estimated.

The pulsar proper motion was estimated by Ferraro et. al (2012) to be  $\mu_{\alpha \cos(\delta)} = 3.82 \pm 0.62 \text{ mas yr}^{-1}$  and  $\mu_{\delta} = 2.13 \pm 0.23 \text{ mas yr}^{-1}$ . The magnitude of the system in STmag magnitude system was calculated to be  $m_{F435W} = 27.0$  and  $m_{F606W} = 28.3$ . Using the following relation,  $\text{mag}_{\lambda} = -2.5 \log F_{\lambda} - 21.1$ , the spectral flux was calculated to be  $F_{F435W} = 8.7 \times 10^{-5} \text{ keV cm}^{-2} \text{ s}^{-1}$  and  $F_{F606W} = 4.2 \times 10^{-5} \text{ keV cm}^{-2} \text{ s}^{-1}$ . These spectral fluxes were then used to constrain the spectral model mentioned earlier.

To constrain the spectral model suggested by X-ray analysis, the power law and black-body components were extended into the optical range. Only the extrapolated cold black-body component was in agreement with the optical measurements (figure 5). The spin

down luminosity of pulsar A being three orders of magnitude higher than that of B ( as discussed by Lyne et al. (2004)), the optical emission is expected to be magnetospheric emission from pulsar A. From the extrapolation, it was thus concluded by Ferraro et. al (2012) that either the pulsar A magnetosphere does not provide any contribution in the non-thermal region or there is a break at these wavelengths. The spectral model of power law and two blackbody components as predicted by the XMM-Newton data would comply with the optical study only in the case of a spectral break at low energies in the power law component. Such a spectral break was observed by Mignani et al. (2014) in many pulsars, and is thus a possibility. It was expected that observations in UV will be possible that will allow making better constraints on the thermal emission from the system.

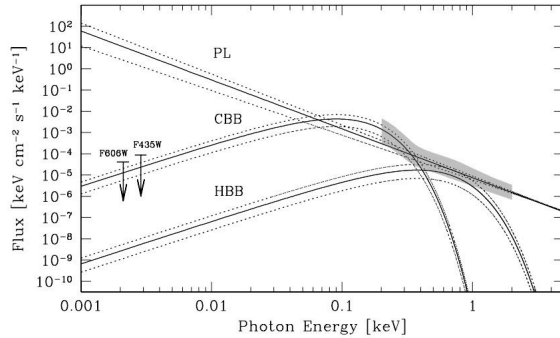


**Figure 5.** Extrapolation into the optical regime of the model that best fits the XMM-Newton data of the pulsar system: a cooler BB and a hotter BB plus a PL. The solid lines are the best-fit model components, while the dot-dashed lines correspond to the 90% confidence level uncertainties of the best fit. The gray region marks the location and uncertainties of the X-ray measurements. The two arrows indicate the F435W- and F606W-band upper limits obtained from the HST data. Image and description taken from Ferraro et. al (2012)

The system was observed in the FUV using Solar Blind Channel of ACS aboard the HST by Durant et al. (2014). Low-pass filter F125LP was used to make these observations. As with the optical analysis, the extrapolated power law component from X-Ray observations overshoots the UV measurements (figure 6). This again hints at a power law spectrum that breaks at lower energies. Additionally, after taking the observed reddening into account ( $E(B-V)=0.1$ ), a temperature of 0.4 MK was obtained. However, applying this to the X-ray model yielded an emitting radius of around 33 km. It was significantly more than the expected value, and it was thus concluded that the three component spectral model predicted by X-Rays could indeed be incomplete. A final statement about the validity of the model could not be made before further observations in UV and optical are made.



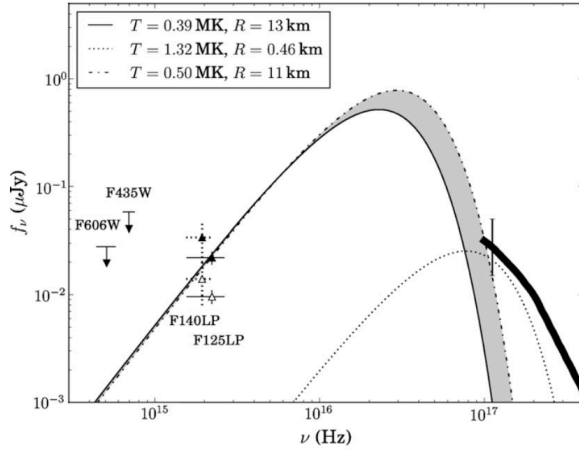


**Figure 6.** Measurements and models for the spectral flux of J0737. The unfilled and filled triangles show the measured and extinction-corrected FUV fluxes, respectively, in the F125LP and F140LP filters for  $E(B - V) = 0.1$ . The upper limits in two optical filters are from Ferraro et. al (2012). The unabsorbed X-ray spectrum taken from Pellizzoni et al. (2008) is shown by the thick line; the dotted line shows the cold BB component from the BB+BB model for the phase-integrated X-ray spectrum. The solid and dashed lines show examples of BB models which best fit the F125LP detection for  $E(B - V) = 0.1$ . The radii in the legend are for  $d = 1.1$  kpc. Image and description taken from Durant et al. (2014)

#### 4. X-Ray

The pulsed emission from pulsar B could no longer be detected after 2008, as reported by Perera et al. (2010). It was proposed that pulsar B would be visible by 2014 if a bipolar beam shape is assumed, but analysis by Lomiashvili and Lyutikov (2014) showed that depending on the beam shape, the pulsar B should reappear in 2034, 2043, or 2066. The prevalent models were thus unable to explain the disappearance of pulsar B. Even before that, the pulse variability and eclipsing of pulsar A were attributed by Lyne et al. (2004) to magnetospheric-wind interactions in the pulsar system which could not be completely characterized using only radio observations. X-ray observations were thus required to study the magnetospheric properties of the pulsar binary system.

The first X-ray observations came from Chandra’s Advanced CCD Imaging Spectrometer analyzed by McLaughlin et al. (2004). The 0.2–10 keV luminosity was found to be  $L_x = 2 \times 10^{30} \text{ erg s}^{-1}$  at a distance of 0.5 kpc. The photon index was reported to be  $\Gamma = 2.9 \pm 0.4$ . It was speculated that the X-Ray emission was coming from magnetosphere of pulsar A. Alternatively, it was proposed that relativistic winds of pulsar A and pulsar B colliding lead to X-ray emission. However, further study was required to make more definite statements about the magnetospheric properties of the pulsar system.

To further constrain the high-energy emission spectrum of the system and get a better insight into the flux variability of the source, Pellizzoni et al. (2004) studied PSR J0737–3039 using XMM-Newton’s European Photon Imaging Camera (EPIC). The data collected fitted well to an absorbed power-law model with  $\Gamma = 3.5^{+0.5}_{-0.3}$  and an absorption of  $N_H = (7.0 \pm 2.5) \times 10^{20} \text{ cm}^{-2}$ . The data also satisfied a bremsstrahlung model with a temperature of  $0.5 \pm 0.1 \text{ keV}$  and  $N_H < 5 \times 10^{20} \text{ cm}^{-2}$ . A blackbody (BB) plus a power law (PL) model was also applied which fit to the data at  $\Gamma = 2$ . Pellizzoni et al. (2004) compared the results obtained with other millisecond pulsars and concluded that a composite spectrum

was the most plausible model to go with. While the thermal component was predicted to be possibly coming from pulsar A, the non-thermal component was speculated to be from particle acceleration at the bow shocks due to magnetospheric interactions between the two pulsars as suggested by Granot and Mszros (2004). One definite spectral model could still not be determined, though. Pellizzoni et al. (2004) were also not able to get significant data on pulsating x-ray emission.

The first pulsed emission in X-rays were detected by Chatterjee et al. (2007) using Chandra's High Resolution Camera (HRC-S) for observations spanning 10.5 orbits.

## References

- Burgay, M., N. D'Amico, A. Possenti, R. N. Manchester, A. G. Lyne, B. C. Joshi, M. A. McLaughlin, et al. 2003. *Nature* 426 (6966): 53133. <https://doi.org/10.1038/nature02124>.
- Lyne, A.G., 2006. *Chinese Journal of Astronomy and Astrophysics Supplement* 6, 162.
- Lyne, A.G., Burgay, M., Kramer, M., Possenti, A., Manchester, R.N., Camilo, F., McLaughlin, M.A., Lorimer, D.R., D'Amico, N., Joshi, B.C., Reynolds, J., Freire, P.C.C., 2004. *Science* 303, 11531157.
- Kramer, M., Wex, N., 2009. *Class. Quantum Grav.* 26, 073001.
- Kaspi, V.M., Ransom, S.M., Backer, D.C., Ramachandran, R., Demorest, P., Arons, J., Spitkovsky, A., 2004. *The Astrophysical Journal* 613, L137L140.
- Lyutikov, M., Thompson, C., 2005. *ApJ* 634, 1223.
- Arons, J., C. Backer, D., Spitkovsky, A., M. Kaspi, V., 2005. 95.
- James Justin Condon, Scott M. Ransom, 2016. 6 Pulsars Essential Radio Astronomy [WWW Document]. URL <https://www.cv.nrao.edu/~sransom/web/Ch6.html> (accessed 10.17.18).
- Lipunov, V.M., 2004. arXiv:astro-ph/0406502.
- Ferraro, F.R., Mignani, R.P., Pallanca, C., Dalessandro, E., Lanzoni, B., Pellizzoni, A., Possenti, A., Burgay, M., Camilo, F., D'Amico, N., Lyne, A.G., Kramer, M., Manchester, R.N., 2012. *The Astrophysical Journal* 749, 84.
- Pacini, F., 1971. *The Astrophysical Journal* 163, L17L19.
- Pacini, F., Salvati, M., 1987. *The Astrophysical Journal* 321, 447.
- Pellizzoni, A., Tiengo, A., De Luca, A., Esposito, P., Mereghetti, S., 2008. *The Astrophysical Journal* 679, 664674.
- Mignani, R.P., Corongiu, A., Pallanca, C., Oates, S.R., Yershov, V.N., Breeveld, A.A., Page, M.J., Ferraro, F.R., Possenti, A., Jackson, A.C., 2014. *Monthly Notices of the Royal Astronomical Society* 443, 22232241.
- Durant, M., Kargaltsev, O., Pavlov, G.G., 2014. *The Astrophysical Journal* 783, L22.
- Perera, B.B.P., McLaughlin, M.A., Kramer, M., Stairs, I.H., Ferdman, R.D., Freire, P.C.C., Possenti, A., Breton, R.P., Manchester, R.N., Burgay, M., Lyne, A.G., Camilo, F., 2010. *ApJ* 721, 1193.
- Breton, R.P., Kaspi, V.M., Kramer, M., McLaughlin, M.A., Lyutikov, M., Ransom, S.M., Stairs, I.H., Ferdman, R.D., Camilo, F., Possenti, A., 2008. *Science* 321, 104107.
- Lomiashvili, D., Lyutikov, M., 2014. *Mon Not R Astron Soc* 441, 690714.
- McLaughlin, M.A., Camilo, F., Burgay, M., D'Amico, N., Joshi, B.C., Kramer, M., Lorimer, D.R., Lyne, A.G., Manchester, R.N., Possenti, A., 2004. *The Astrophysical Journal* 605, L41L44.
- Pellizzoni, A., Luca, A.D., Mereghetti, S., Tiengo, A., Mattana, F., Caraveo, P., Tavani, M., n.d. 612, 4.
- Granot, J., Mszros, P., 2004. *The Astrophysical Journal* 609, L17.
- Chatterjee, S., Gaensler, B.M., Melatos, A., Briskin, W.F., Stappers, B.W., 2007. *The Astrophysical Journal* 670, 1301.